

# Beam collimation in the transfer line from 8 GeV linac to the Main Injector\*

A.I. Drozhdin

*Fermi National Accelerator Laboratory*

*P.O. Box 500, Batavia, Illinois 60510*

September 8, 2004

## 1 Beam parameters and assumptions

Proton momentum  $P = 8.88889 \text{ GeV}/c$ ,

95% normalized emittance of the beam in the transfer line is  $\epsilon = 1.5 \pi \text{ mm} \cdot \text{mrad}$ ,

Momentum collimation in the beam transfer line is done at  $dP/P = 0.98 \cdot 10^{-3}$ .

Painting injection to the Main Injector lasts 270 turns, and accumulated intensity of the circulating beam is  $1.5 \times 10^{14} \text{ ppp}$ . Emittance of the beam after painting is  $\epsilon = 40 \pi \text{ mm} \cdot \text{mrad}$ . Main Injector repetition rate is 0.67 Hz. Extracted beam power ( $10^{14} \text{ prot/sec}$  at 120 GeV) is 1.9 MW.

## 2 Lattice for momentum collimation

Off-momentum collimation can be done in two or in one location of the beam line:

- In a first case off-momentum beam should have a displacement in the collimators by a half-size of the beam and phase advance between collimators must be equal to  $\pi$ , if dispersion has the same sign in both locations, or  $2\pi$ , if dispersion has different signs in the locations of collimators (Fig. 1 top and middle).

- In a second case the off-momentum beam should have a displacement in the collimator by a total size of the beam (Fig. 1 bottom). This requires a factor of 2 bigger dispersion and larger aperture of the beam line.

### 2.1 Choice of phase advance per cell

Horizontal  $\beta$  function and dispersion in the  $45^\circ$ ,  $60^\circ$  and  $90^\circ$  phase advance per cell achromatic lattices are shown in Fig. 2. This kind of lattice may be used for off-momentum collimation by two stripping foils located at  $3\sigma_x$  from both sides of the beam in two places with positive and negative dispersion, located at phase advance of  $2\pi$  between them (two-wave dispersion lattice). Displacement of off-momentum particles  $dX$  should be bigger than  $3\sigma_x$  of the beam. As shown here the  $45^\circ$  and  $60^\circ$  lattices have much smaller beta compared to the  $90^\circ$  lattice for the same amount of dispersion and total length. This is an advantage for off-momentum collimation. Parameters of beam lines with different phase advance per cell are presented in Table 1.

---

\*Work supported by the Universities Research Association, Inc., under contract DE-AC02-76CH00300 with the U. S. Department of Energy.

phase advance per cell ( $\psi$ )	dispersion ( $\eta$ )	$dX = \eta \cdot dP/P$	$\beta_x$	$3\sigma_x$	beam line length
degree	m	mm	m	mm	m
Two-wave dispersion beam line					
45	8.88	10.0	69.0	8.1	585.75
60	8.85	10.0	76.9	8.5	560.88
90	8.80	9.9	110.2	10.2	528.76

Table 1: Parameters of beam lines with different phase advance per cell. 95% emittance is  $\epsilon = 6.0 \pi \text{ mm} \cdot \text{mrad}$ .

## 2.2 Comparison of lattices with one and two waves of dispersion

The  $\beta$  functions and dispersion in a  $60^\circ$  phase advance per cell achromatic lattice are shown in Fig. 3. This lattice is used for off-momentum collimation by two stripping foils located at  $3\sigma_x$  from both sides of the beam in only one place of the beam line (one-wave dispersion lattice). Displacement of off-momentum particles  $dX$  should be bigger than  $6\sigma_x$  of the beam. Comparison of one and two dispersion wave lattice parameters are presented in Table 2 for beam emittance of  $\epsilon = 6.0 \pi \text{ mm} \cdot \text{mrad}$  and  $\epsilon = 1.5 \pi \text{ mm} \cdot \text{mrad}$ .

phase advance per cell ( $\psi$ )	beam emittance	dispersion ( $\eta$ )	$dX = \eta \cdot dP/P$	$\beta_x$	$3\sigma_x$	beam line length
degree	$\text{mm} \cdot \text{mrad}$	m	mm	m	mm	m
One-wave dispersion lattice						
60	6.0	19.8	22.3	115.3	10.4	420.66
60	1.5	9.43	10.6	89.3	4.58	313
Two-wave dispersion lattice						
60	6.0	8.85	10.0	76.9	8.5	560.88
60	1.5	4.85	5.46	66.3	3.97	467

Table 2: Comparison of beam lines for off-momentum collimation with one and two waves of dispersion. Two values of 95% emittance are used:  $\epsilon = 6.0 \pi \text{ mm} \cdot \text{mrad}$  and  $\epsilon = 1.5 \pi \text{ mm} \cdot \text{mrad}$ .

## 3 Total transfer beam line

Starting from this section we assume that “two-wave dispersion lattice” is used for collimation. That does not mean that this is a final decision. If solution is different, the calculations will be done again and this will result only the length and aperture of beam line without difference in other conclusions of this work.

We assume here also that the same  $60^\circ$  phase advance FODO lattice is used for amplitude and momentum collimation. The amplitude collimation section consists of three FODO cells without dipole magnets. The momentum collimation section consists of six FODO cells with positive field dipole magnets and six cells with negative field magnets.

The total beam line is combined of five sections: section for matching of the beam parameters between Linac exit and the FODO lattice of the beam line, momentum jitter correction section, amplitude collimation, momentum collimation, matching between FODO lattice of the beam line and the Main Injector MI10 straight section. The  $\beta$  functions, horizontal dispersion and 3- $\sigma$  beam

size in the beam transfer line are shown in Fig. 4.

Possibly, the momentum jitter correction can be combined with the momentum collimation because of similar requirements to the dispersion and beam size at the location of the system. Nevertheless the less the radiation conditions and required space for the equipment of jitter compensation system may be the problems to do this combination. The beam line with combination of jitter correction and momentum collimation in one section allows to decrease the total beam line length from 883 m to 649 m (Fig. 5).

Based on this calculations we may conclude that there are two possible solutions for collimation of the beam before injection to the Main Injector: first to use two-wave dispersion lattice 467 m long with aperture of D24 mm, second - to use one-wave dispersion lattice 353 m long (with additional matching section of  $\sim 40$  m long) with aperture of D37 mm. The total length of two-wave lattice is 649 m, and one-wave lattice length is 546 m.

## 4 Beam line location with respect to the Antiproton Target Hall

The transfer beam line trajectory should miss the existing Antiproton Target Hall located at this region. Different configurations (A,B,C,D) of beam line which correspond to different position of transfer beam line with respect to the Antiproton Target Hall are shown in Fig. 6 with separate section for jitter correction, and in Fig. 7 with jitter correction and momentum collimation combined in the same section. In the first two top cases, shown in both figures, the amplitude collimation is upstream of the momentum collimation section. In the last two cases amplitude collimation is in the middle of the momentum collimation section. As the phase advance in the amplitude collimation section is equal to  $\pi$  this permits to have the same sign of magnet field in both parts of momentum collimation section in the two bottom cases.

The top view of beam line orbits (footprints) with separate section for jitter correction and jitter correction combined with momentum collimation in the same section are shown in Fig. 8. As shown in Fig. 9, versions D and C do not satisfy the requirements as their trajectories pass through the Antiproton Target Hall.

## 5 Magnetic stripping of $H^-$ ions in the beam transfer line

The stripping of  $H^-$  ions by the magnetic field of elements of beam transfer line (Lorentz stripping) was calculated using equation (M.A.Furman) for ion's lifetime in its own rest frame system:

$$\tau = \frac{A}{E} \exp\left(\frac{C}{E}\right) \quad (1)$$

Here  $E[MV/cm] = 3.197 \times P[GeV/c] \times B[T]$

In a range of  $E[MV/cm] = 1.87 - 2.14$   $A = 7.96 \times 10^{-14} s \cdot MV/cm$  and  $C = 42.56 MV/cm$ .

The mean decay length in the lab system is given by

$$\lambda = c\beta\gamma\tau \quad (2)$$

The stripping probability was calculated as  $p_{strip} = l/\lambda$

Here  $l$  is a magnetic length of the element.

A sum of stripping probabilities at each element of beam line for every particle of a  $3\sigma$  beam was calculated along the beam line. According to these calculations an average stripping probability is equal to  $2.25 \times 10^{-7}$  at the total length of beam transfer line or  $5 \times 10^{-10} m^{-1}$  in the bend region

of beam line. The stripping probability in a 5.4 m long ( $B=0.05$  T) dipole magnet ( $p_{strip} = 3.2 \times 10^{-9}$ ) is a several order of magnitude higher compared to it in the quadrupole magnet ( $B=0.05$  T at  $R=2.5$  cm).

At the beam intensity of  $10^{14}$  *prot/sec* the beam power is 142 KW and power of particles lost along the beam line because of magnetic stripping is 0.030 W.

## 6 Beam line collimation system

The  $\beta$  functions, horizontal dispersion and  $3\text{-}\sigma$  beam size in the beam transfer line (version A) are shown in Fig. 10. Halo collimation is done by stripping of  $H^-$  ions at the foil located upstream of the focusing quadrupole and then intercepting of the  $H^o$  atoms and protons by the beam dump located in 4 m behind the focusing quadrupole (Fig. 11). The stripping foils and beam dumps are shown by a vertical bars directed down in Fig. 10.

At these simulations the initial beam 95% emittance (including halo) is equal to 4.17 mm-mrad (size of halo is a factor of 5/3 of the design beam size) and  $\sigma_{dp/p}$  of momentum distribution is 0.001. A  $3\sigma_{x,y}$  of the beam is 3.9 mm at the amplitude foils and 3.6 mm at the beam dumps. Collimation of the beam is done with amplitude foils and beam dumps located at 4 mm from the beam center. Momentum collimating foils and beam dumps are at 5 mm from the beam center. Horizontal dispersion at the foil location is  $D=5.1$  m, and  $3\sigma_x$  is 3.9 mm. This provides collimation of the beam at  $dP/P = 0.98 \cdot 10^{-3}$ .

The beam population, including halo, and  $3\sigma$  core of the beam are presented on the left side of Fig. 12 and 13 without collimation. On the right side of these figures the beam population after collimation at every  $60^\circ$  and intercepted halo at the beam dumps are shown. Two bottom rows at Fig. 13 show the beam at the off-momentum beam dumps.

Calculated horizontal, vertical and momentum distributions of the beam without and with collimation are shown in Fig. 14 at the entrance to the MI-10 straight section of the Main injector.

The MARS15 calculations (N.V.Mokhov) on instantaneous temperature rise per a single pulse of  $1.5e14$  protons accidentally lost in iron and aluminum collimators are shown in Fig. 15. It seems iron collimator will withstand a single pulse but will melt if the next pulse arrives. Aluminum collimator will melt after a single pulse. If we follow the SNS policy that the collimator should withstand two pulses in a row, than the optimal solution would be a 0.5-m long and 10-mm radially thick graphite insert in 1-m long steel collimator.

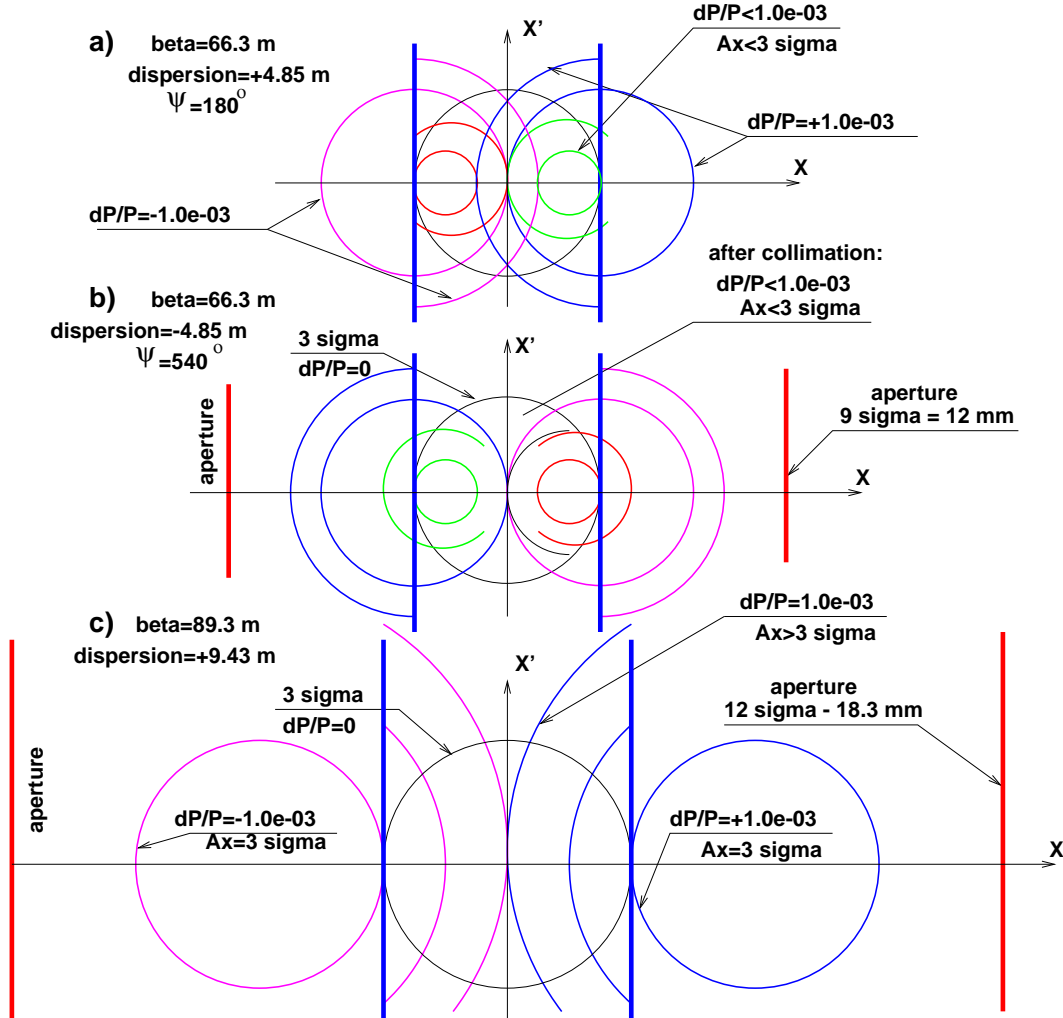


Figure 1: Off-momentum collimation in two locations of beam line: top - in the location with positive dispersion, and middle - in the location with negative dispersion. Bottom - collimation in one location of beam line. As amplitude collimators are located at  $3\sigma$ , the system performs collimation of particles with  $A > 3\sigma$  and  $dP/P > 10^{-3}$  in both cases. Minimal horizontal aperture of the elements is equal to  $6\sigma_x$  in the first case, and  $9\sigma_x$  in the second one. If one assumes a distance between the beam pipe and the edge of the beam equal to  $3\sigma_x$ , the required radius of aperture is equal to  $9\sigma_x$  in the first case, and  $12\sigma_x$  in the second one. This gives the beam pipe diameter of  $24$  mm for the first case, and  $37$  mm for the second one. 95% normalized emittance of the beam is  $\varepsilon = 1.5 \pi \text{ mm} \cdot \text{mrad}$

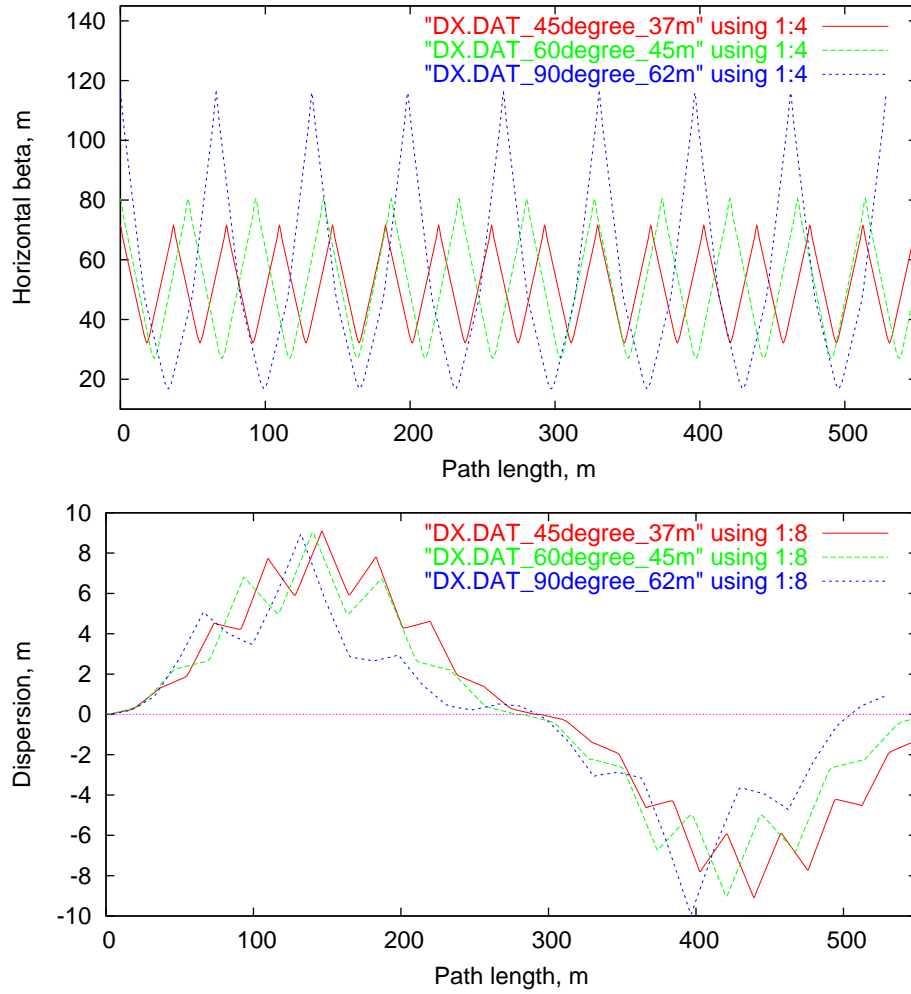


Figure 2: Horizontal  $\beta$  function (top) and dispersion (bottom) in the  $45^\circ$ ,  $60^\circ$  and  $90^\circ$  phase advance per cell achromatic lattices. 16 cells of  $45^\circ$ , 12 cells of  $60^\circ$  and 8 cells of  $90^\circ$  are shown. 95% emittance is  $\epsilon = 6.0 \pi \text{ mm} \cdot \text{mrad}$ .

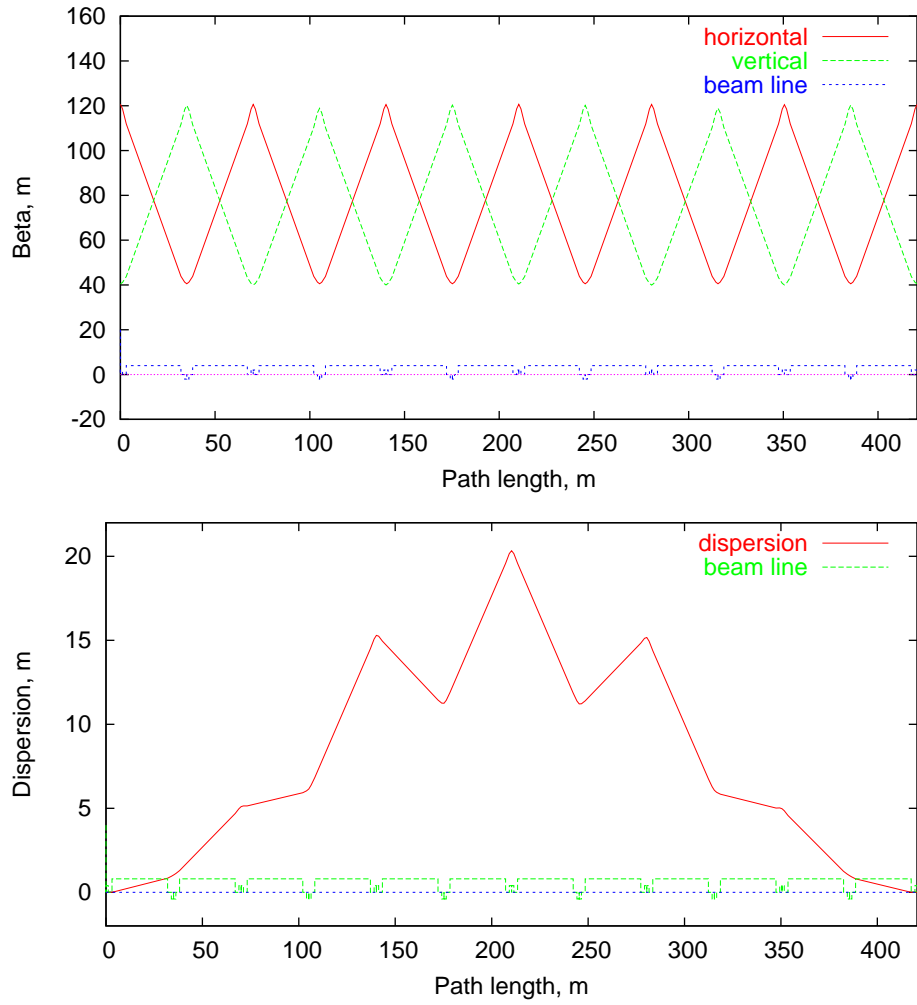


Figure 3:  $\beta$  functions (top) and dispersion (bottom) in the  $60^\circ$  phase advance per cell achromatic lattices. The 95% emittance is  $\epsilon = 6.0 \pi \text{ mm} \cdot \text{mrad}$  here.

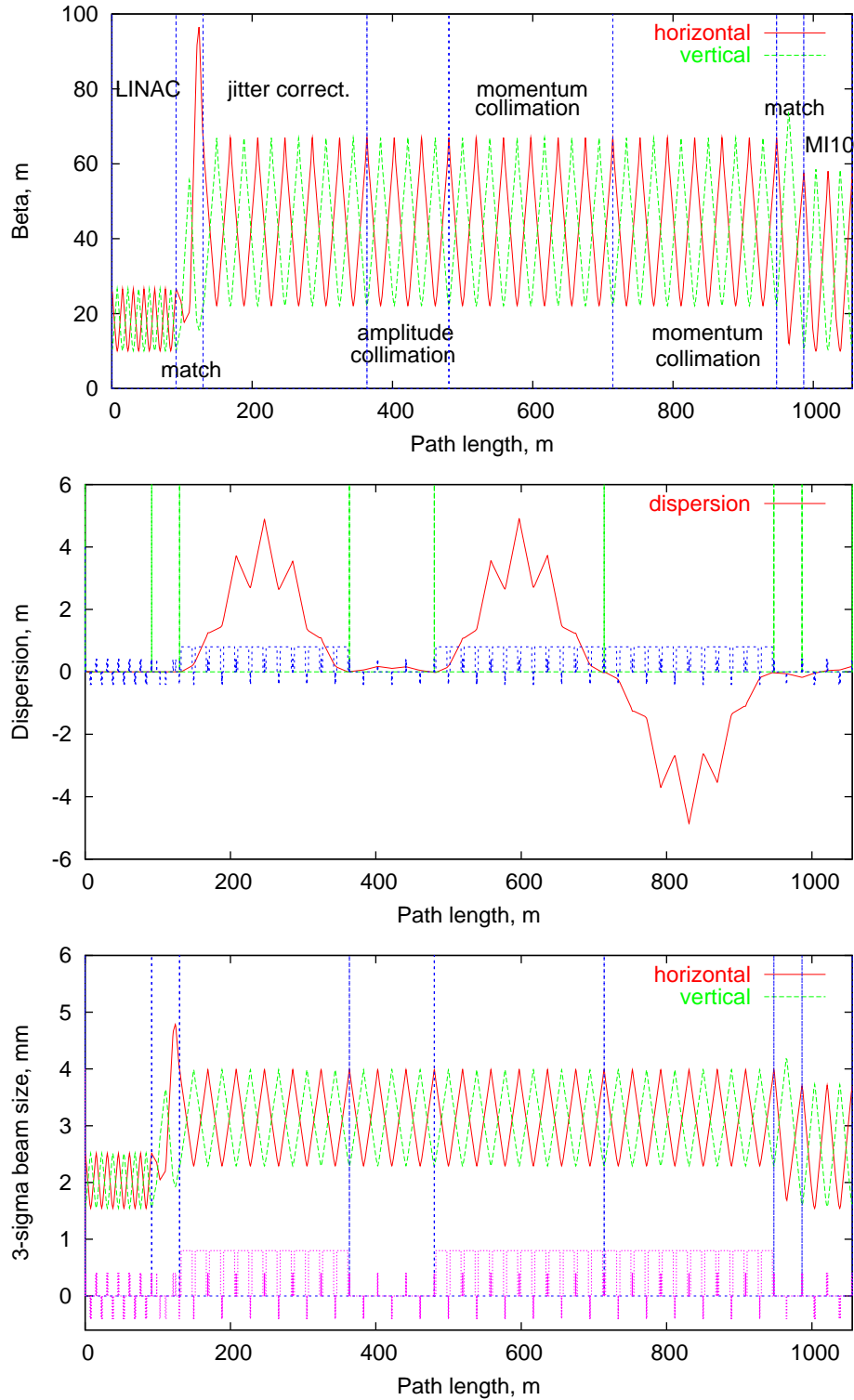


Figure 4:  $\beta$  functions (top), horizontal dispersion (middle) and 3- $\sigma$  beam size in the beam transfer line. Shown here line consists of last six cells of Linac (91.56 m), matching section (26.40 m), jitter correction section (233.64 m), amplitude collimation (116.82 m), momentum collimation (467.28 m), matching section (38.721 m) and Main Injector MI10 straight section (69.158 m). The total length of transfer beam line is 883.061 m.

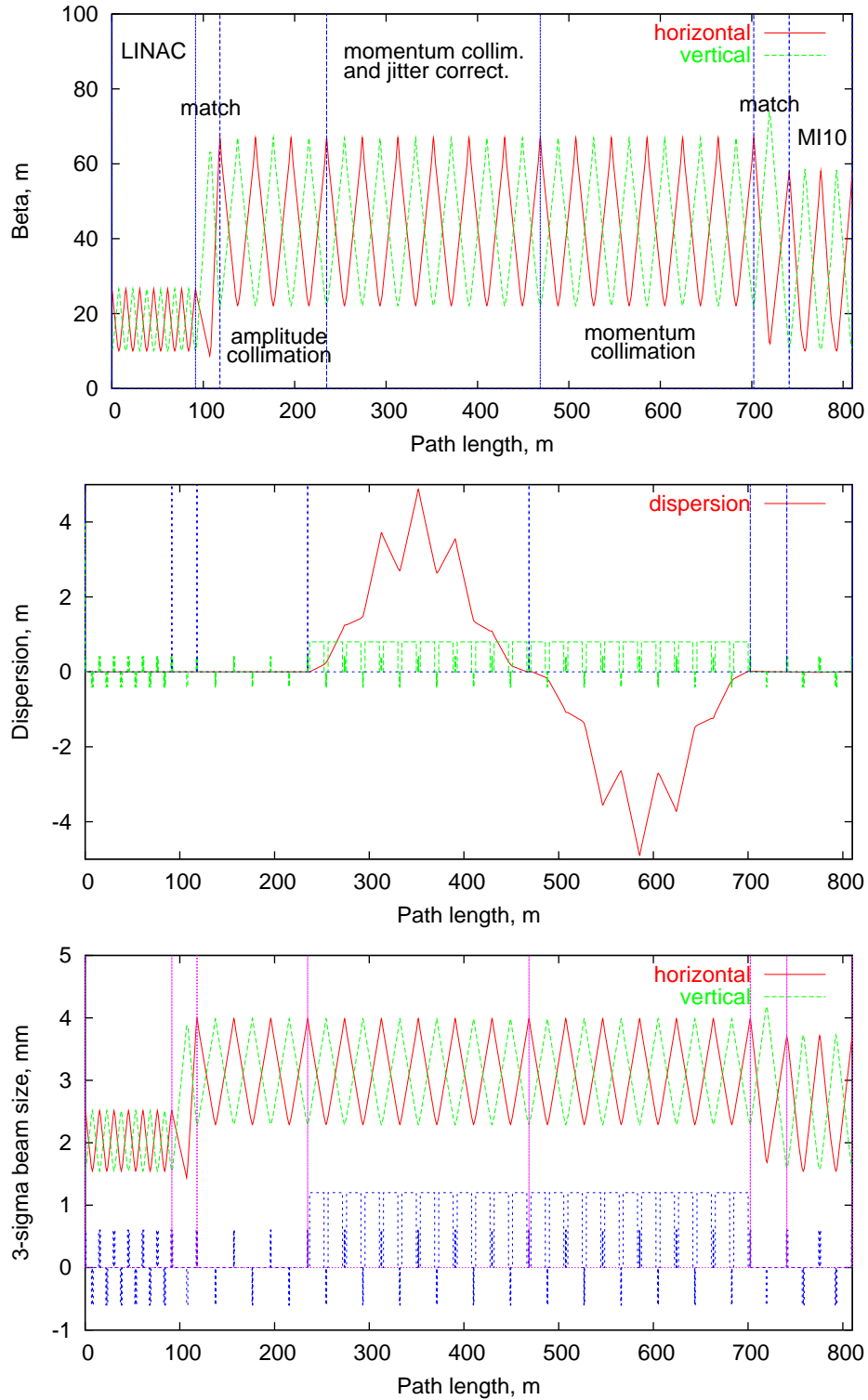


Figure 5:  $\beta$  function (top), horizontal dispersion (middle) and 3- $\sigma$  beam size in the beam transfer line. Shown here line consists of last six cells of Linac (91.56 m), matching section (26.60 m), amplitude collimation (116.82 m), momentum collimation and jitter correction section (233.64 m), second part of momentum collimation (233.64 m), matching section (38.721 m) and Main Injector MI10 straight section (69.158 m). The total length of transfer beam line is 649.421 m

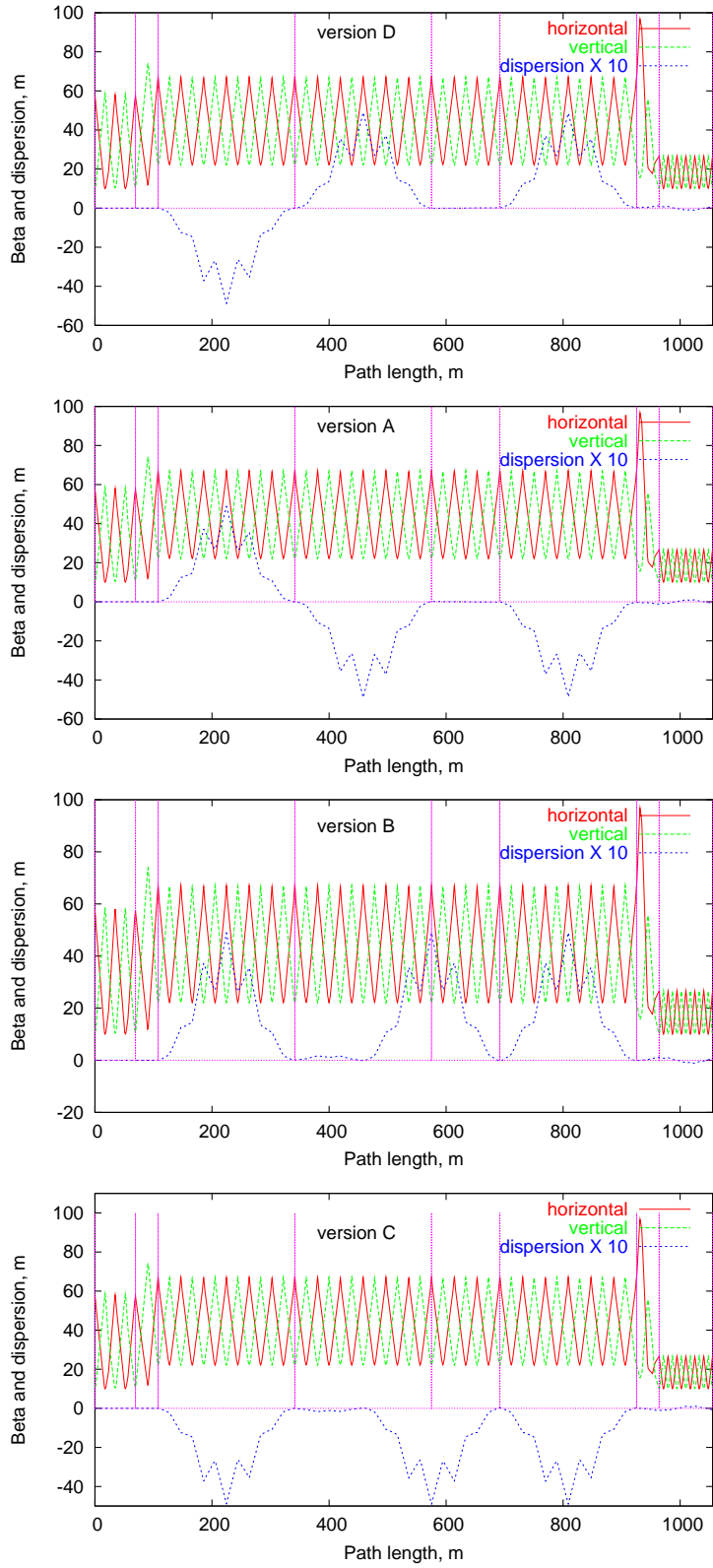


Figure 6: Beta functions and horizontal dispersion in the beam transfer lines with separate section for jitter correction. Different configurations (A,B,C,D) correspond to different position of transfer beam line with respect to the Antiproton Target Hall.

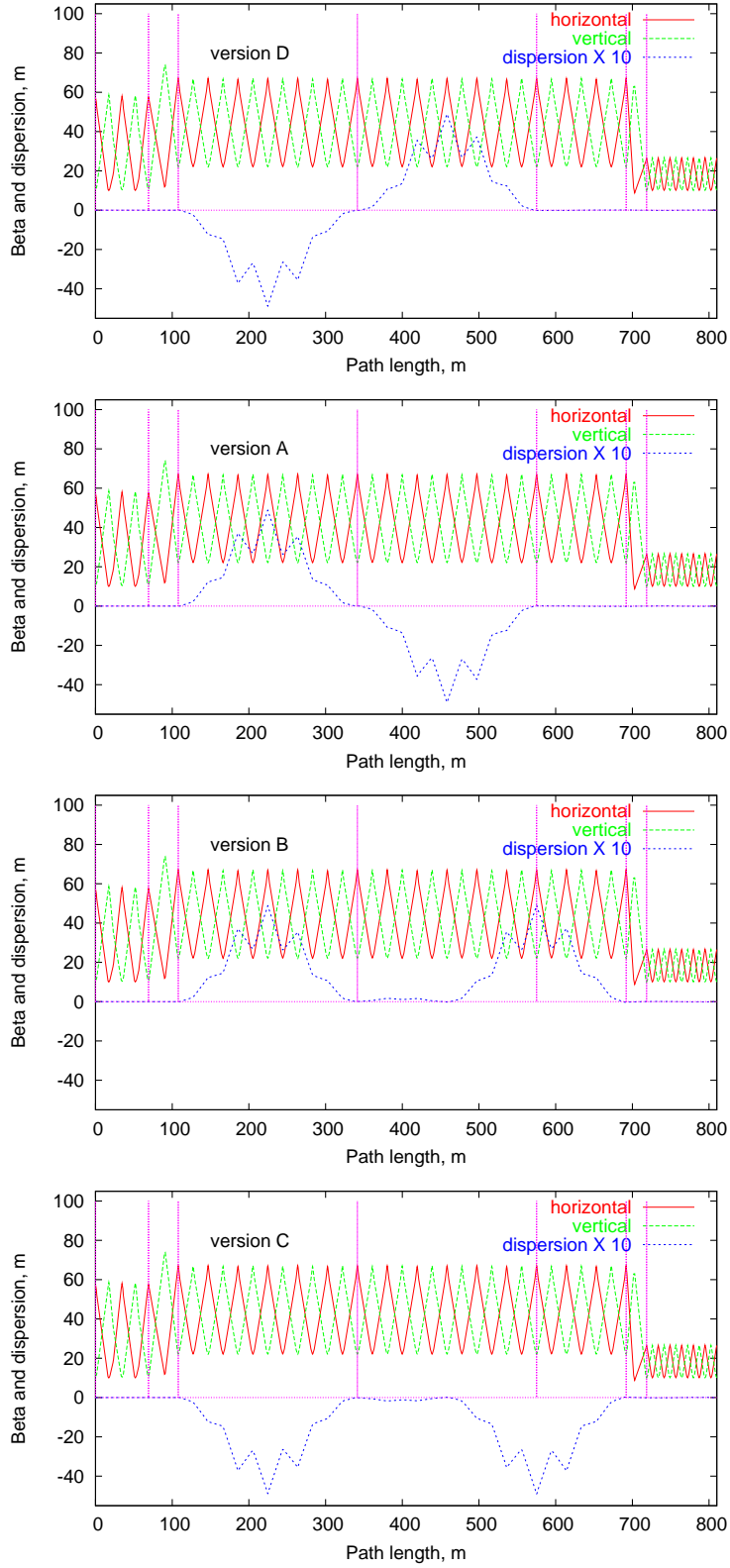


Figure 7: Beta functions and horizontal dispersion in the beam transfer lines with jitter correction and momentum collimation combined in the same section. Different configurations (A,B,C,D) correspond to different position of transfer beam line with respect to the Antiproton Target Hall.

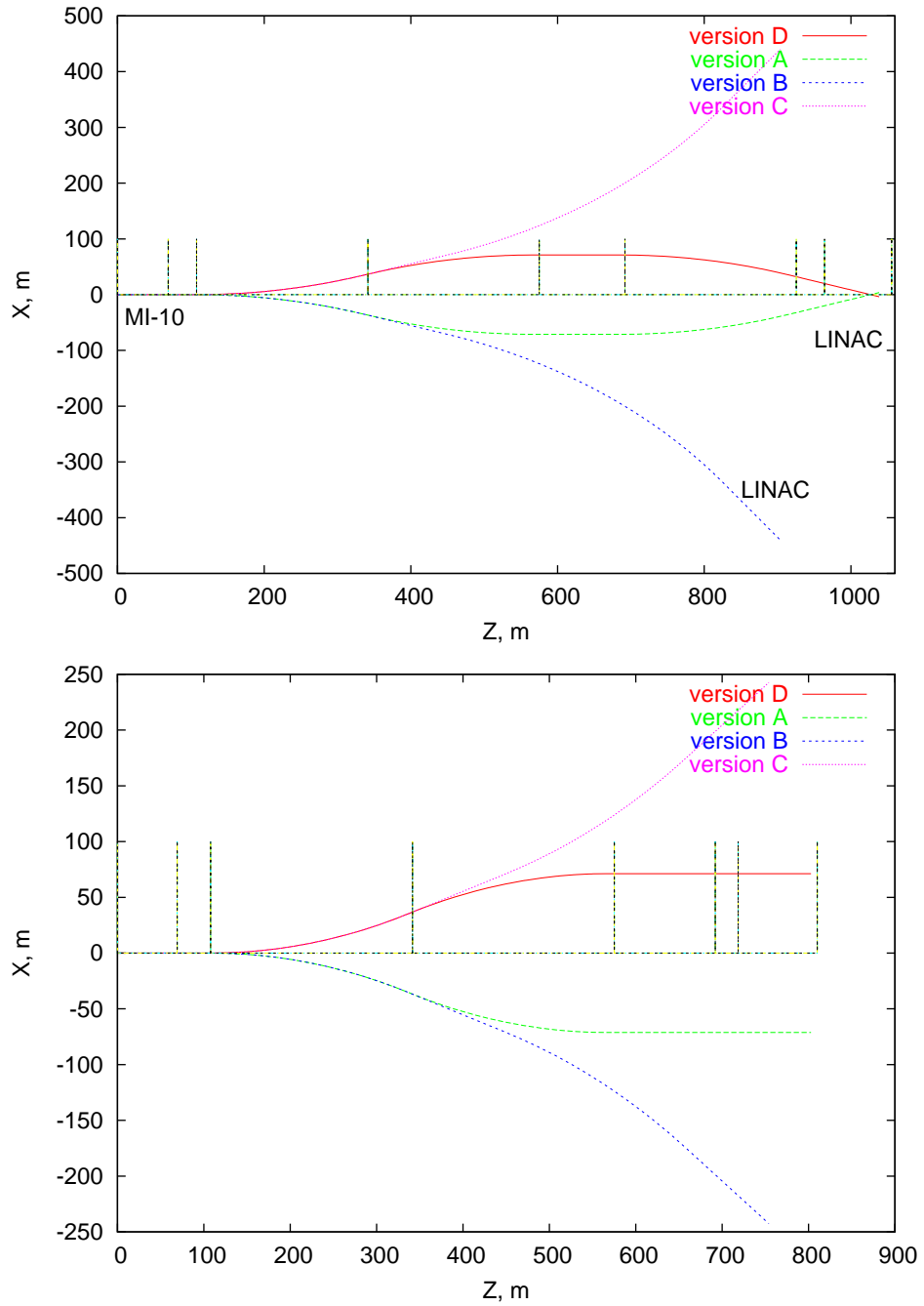


Figure 8: The beam line orbit top view: top - with separate section for jitter correction (233.64 m), bottom - jitter correction is combined with momentum collimation in the same section.

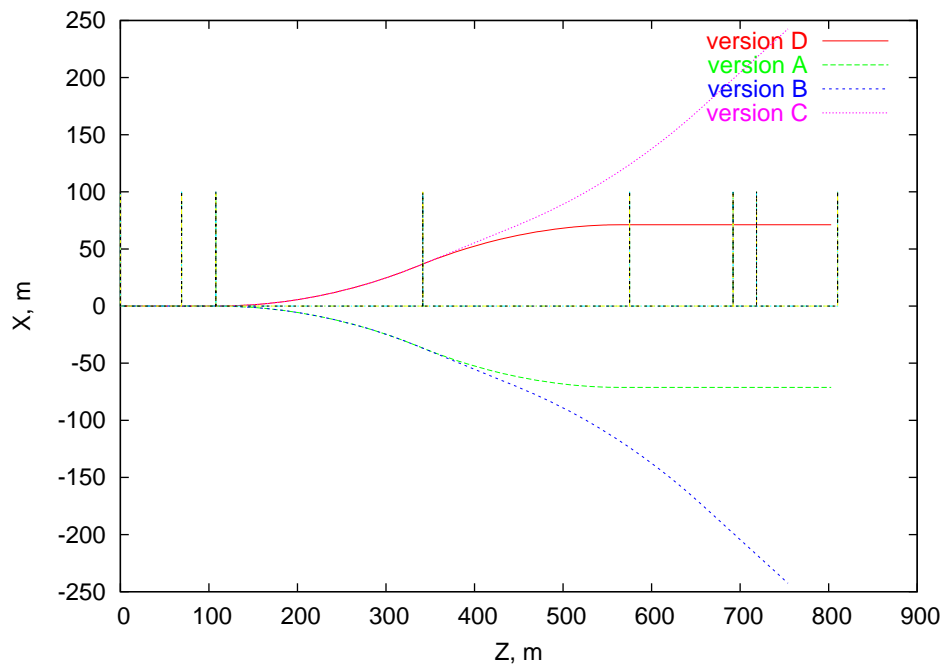


Figure 9: The beam line orbit top view with respect to the Antiproton Target Hall.

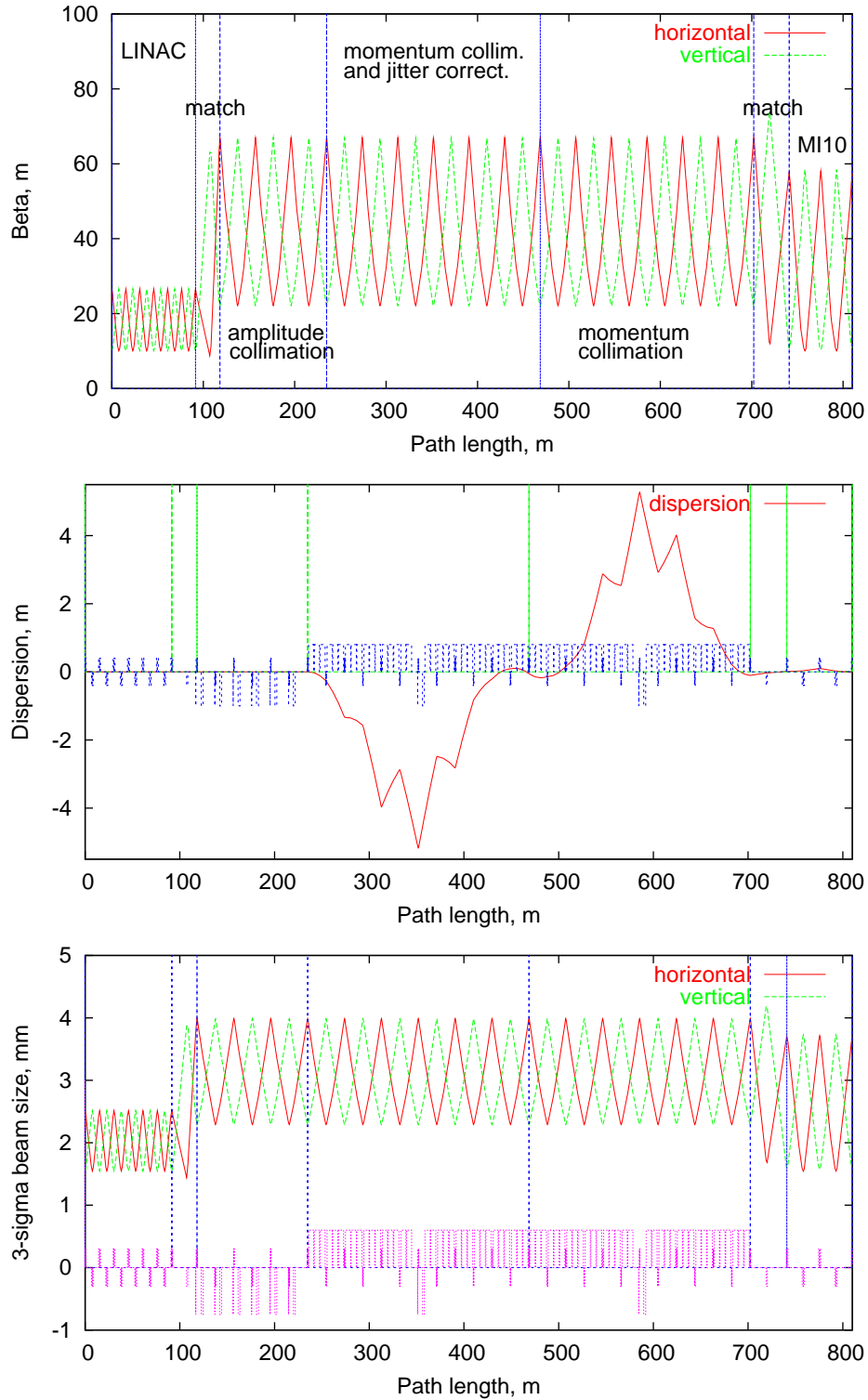


Figure 10:  $\beta$  functions (top), horizontal dispersion (middle) and  $3\text{-}\sigma$  beam size in the beam transfer line (version A). Beam line consists of last six cells of Linac (91.56 m), matching section (26.60 m), amplitude collimation (116.82 m), momentum collimation and jitter correction section (233.64 m), second part of momentum collimation (233.64 m), matching section (38.721 m) and Main Injector MI10 straight section (69.158 m). The total length of transfer beam line is 649.421 m.

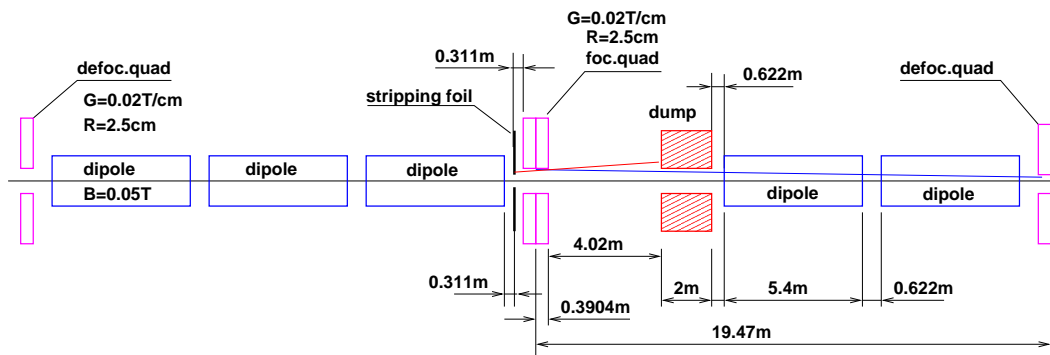


Figure 11: Halo collimation is done by stripping of  $H^-$  at the foil located upstream of the focusing quadrupole and then intercepting of the  $H^o$  atoms and protons at the beam dump located in 4 m behind the focusing quadrupole.

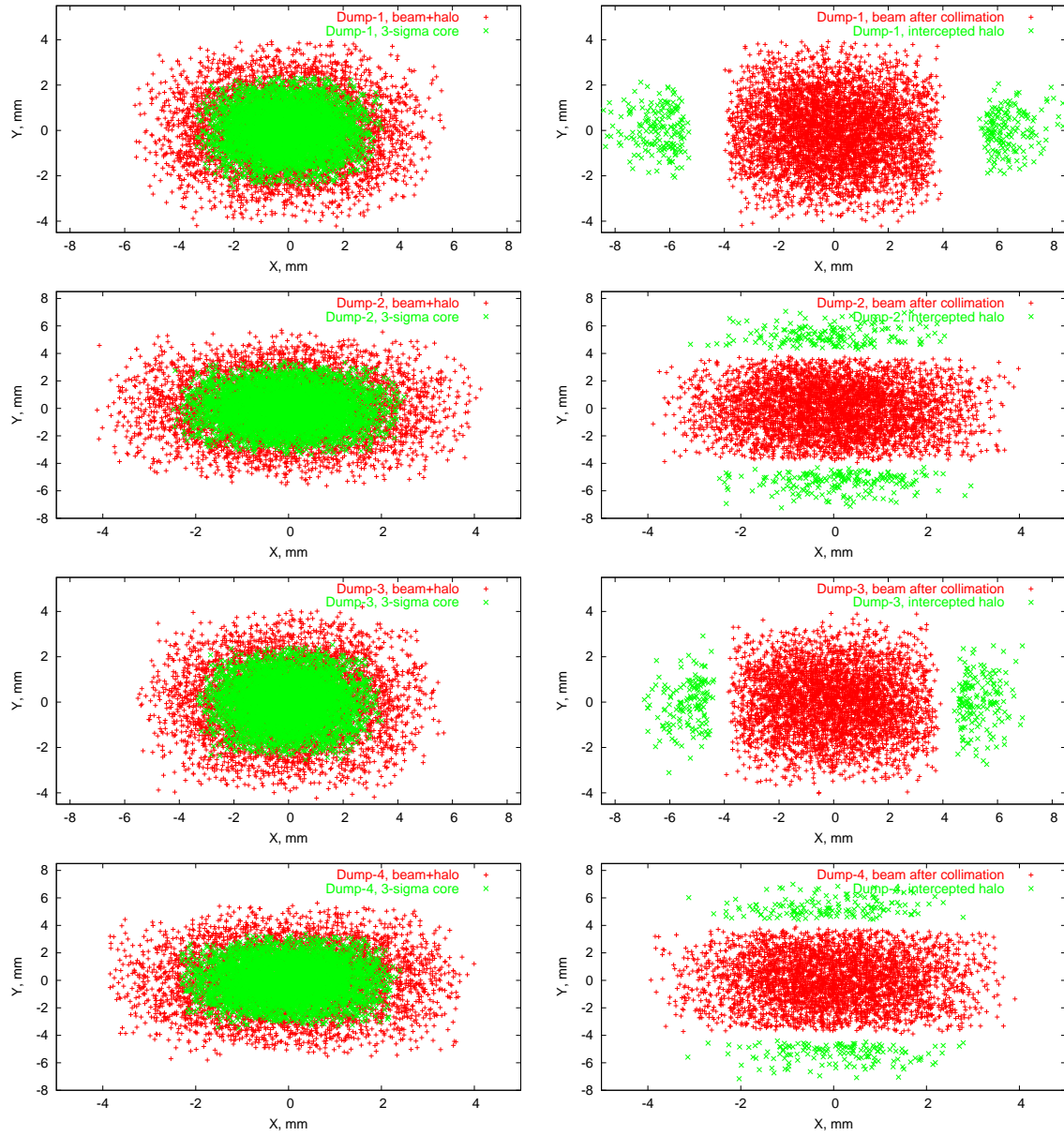


Figure 12: Beam, including halo, without collimation and  $3\sigma$  core (left), and beam after collimation at every  $60^\circ$  and intercepted halo (right) at the beam dump number 1, 2, 3 and 4.

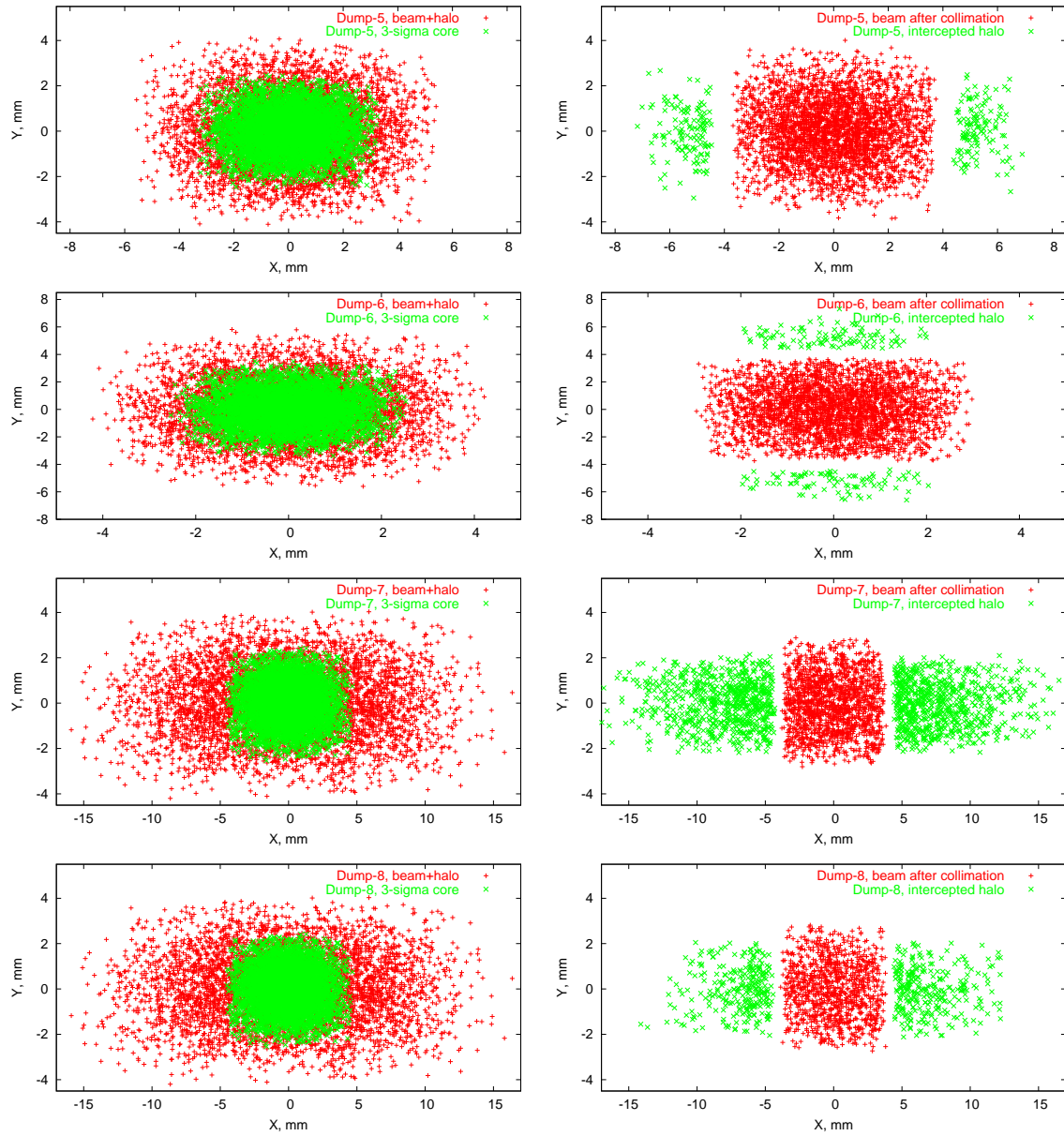


Figure 13: Beam, including halo, without collimation and  $3\sigma$  core (left), and beam after collimation at every  $60^\circ$  and intercepted halo (right) at the beam dump number 5, 6, 7 and 8. Dumps number 7 and 8 are momentum collimating dumps.

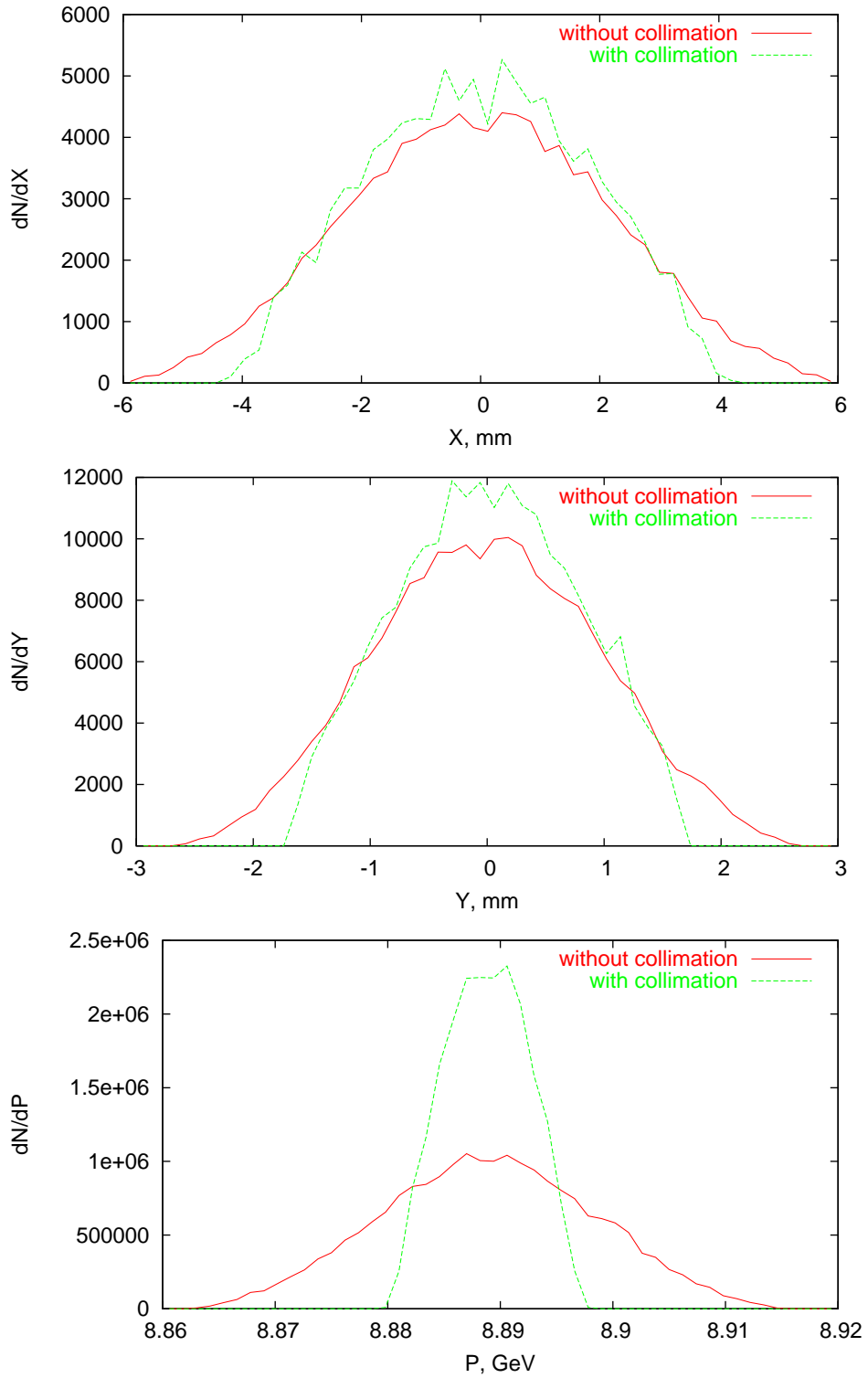


Figure 14: Transverse horizontal (top), vertical (middle) and momentum (bottom) distributions of the beam without and with collimation. Distributions are shown at the entrance to the MI-10 straight section of the Main injector.

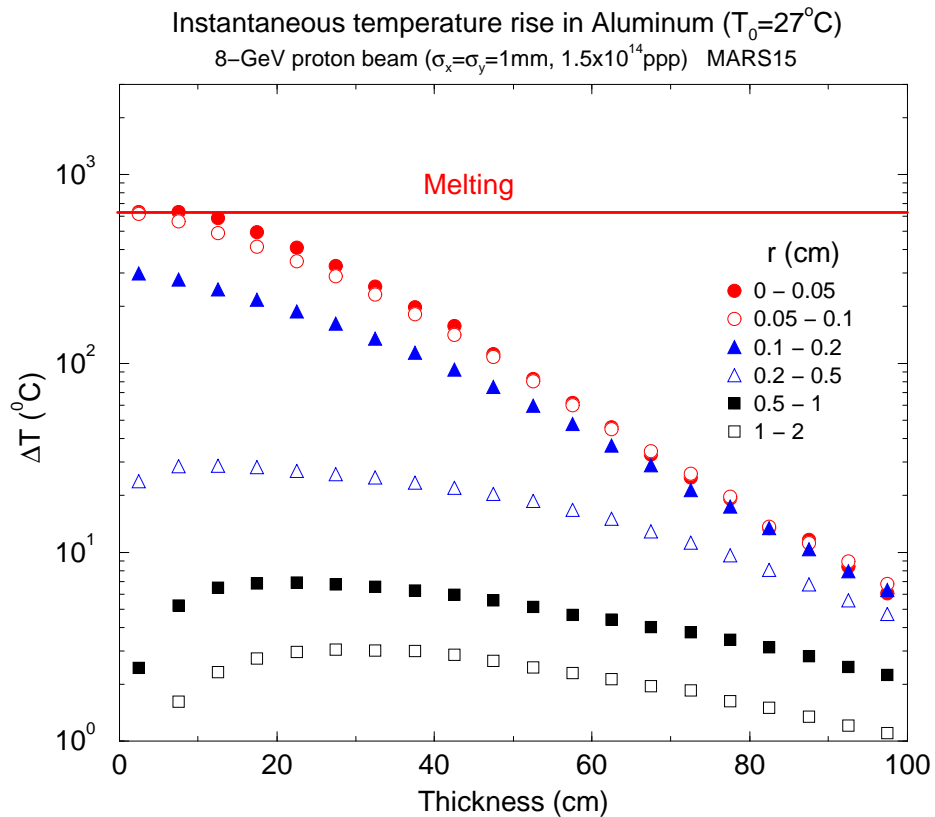
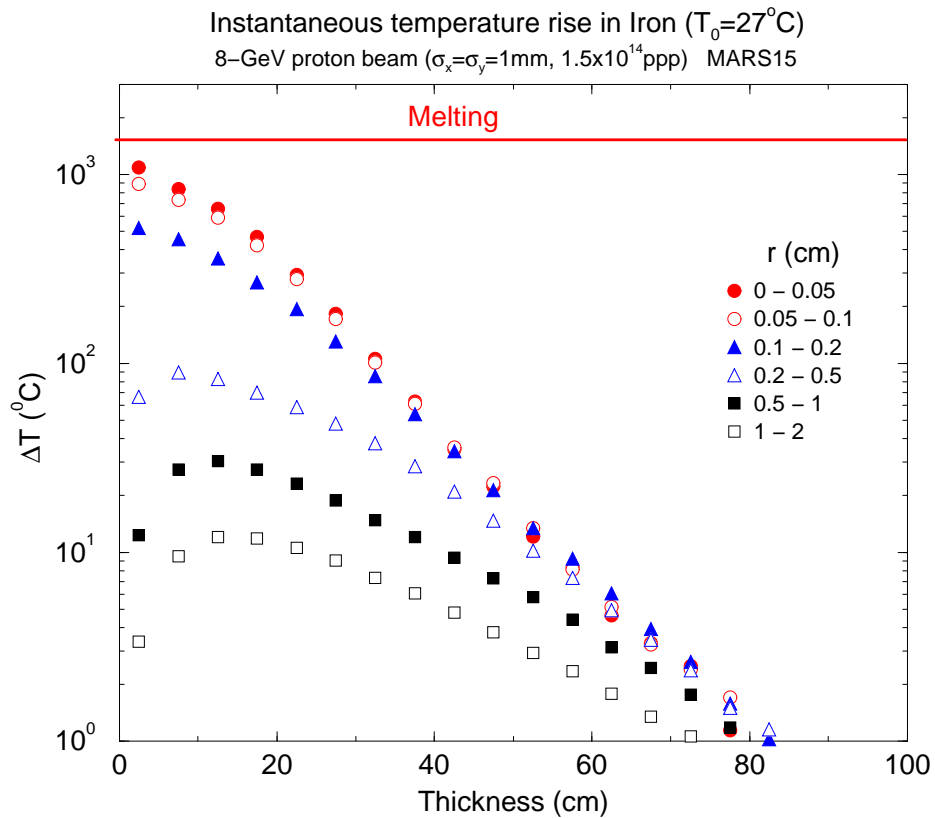


Figure 15: Instantaneous temperature rise per a single pulse of  $1.5\times 10^{14}$  protons accidentally lost in iron (top) and aluminum (bottom) collimators